Atmospheric Environment 62 (2012) 424–432

Contents lists available at SciVerse ScienceDirect

Atmospheric Environment

journal homepage: www.elsevier.com/locate/atmosenv

Aerosol properties over two urban sites in South Spain during an extended stagnation episode in winter season

H. Lyamani [a,b], J. Fernández-Gálvez [a,b,*], D. Pérez-Ramírez [a,b], A. Valenzuela [a,b], M. Antón [a,b], I. Alados [c], G. Titos [a,b], F.J. Olmo [a,b], L. Alados-Arboledas [a,b]

[a] Centro Andaluz de Medio Ambiente, Universidad de Granada, 18006 Granada, Spain
[b] Departamento de Física Aplicada, Universidad de Granada, 18071 Granada, Spain
[c] Departamento de Física Aplicada, Universidad de Málaga, 29071 Málaga, Spain

HIGHLIGHTS

- Study of an intensive and long-lasting aerosol event at regional level.
- Characterization of the atmospheric thermodynamic structure during this event.
- Drastic increase in the aerosol fine concentration during the stagnation episode.
- Increase in modal radius and width of fine particles mode due to growth processes.
- Unusual high single scattering albedo with neutral spectral dependence.

ARTICLE INFO

Article history:
Received 20 January 2012
Received in revised form
16 August 2012
Accepted 24 August 2012

Keywords:
Aerosol size distribution
Aerosol growth
Atmospheric dynamic

ABSTRACT

Columnar and ground level aerosol properties as well as mass concentrations of some gaseous pollutants were measured at two urban sites (Granada and Málaga, South Spain) before, during and after an extended stagnation episode from 7 to 13 February 2011. This long lasting event was associated with a very strong and persistent blocking high-pressure system over the Iberian Peninsula, together with very intense and persistent temperature inversions near the ground level. The columnar aerosol load at Granada showed a significant increase during this stagnation episode as indicated by aerosol optical depth at 440 nm, reaching values four times higher (0.6) than before and after the event. A significant increase in aerosol load at night time was also evidenced by star photometer measurements. Similarly, pronounced enhancement in columnar aerosol load was observed at Málaga, indicating the regional extension of this event. Analysis of ground level measurements obtained at Granada showed a significant increase in aerosol scattering coefficients and aerosol number concentrations during the stagnation episode. Furthermore, the analysis of aerosol size distribution measurements has evidenced the large contribution of fine particles at ground level as well as in the atmospheric column during the stagnation period. The fine mode radius measured at Granada showed a large displacement towards larger sizes together with a pronounced increase in the geometric standard deviation of the fine mode during the high pollution event in the morning hours on 9 February. This was attributed to the growth of aerosol particles due to coagulation and condensation processes as a result of the high fine aerosol load next to the surface favoured by the high pressure system and thermal inversion on that day. This increases in the radius and width of the fine mode results in more efficient scattering in the 440–1020 nm spectral range which, in combination with nearly constant and low imaginary refractive index (0.002) leads to high single scattering albedo with neutral spectral dependency. During the persistent temperature inversion episode the daily European PM_{10} mass concentration limit (50 $\mu g\ m^{-3}$) was exceeded in Granada for most days and in Málaga for three consecutive days. Nevertheless, the mass concentrations of NO_2, CO and O_3 were below the European thresholds with a noticeable decrease in O_3 mass concentration at both sites.

* Corresponding author. Centro Andaluz de Medio Ambiente, Universidad de Granada, Junta de Andalucía, Av. del Mediterráneo s/n, 18006 Granada, Spain. Tel.: +34 958 249751; fax: +34 958 137246.
E-mail address: jesusfg@ugr.es (J. Fernández-Gálvez).

1352-2310/$ – see front matter © 2012 Elsevier Ltd. All rights reserved.
http://dx.doi.org/10.1016/j.atmosenv.2012.08.050

1. Introduction

Air pollution episodes occur in many cities around the world and can pose a serious hazard to human health. Although anthropogenic emissions are the primary cause of atmospheric air pollutants, other factors including meteorological conditions, topography, temperature inversions, atmospheric chemical processes and solar radiation can greatly influence the concentrations of pollutants in the atmosphere (Fisher et al., 2001). In fact, elevated concentrations of atmospheric aerosol and some gaseous pollutants usually occur in urban areas during specific meteorological conditions such as near-surface temperature inversion, high pressure system and low wind (Choi et al., 2008). Throughout peak pollution episodes the mass concentrations of some air pollutants can significantly exceed national and international standards along with threshold values established for protecting human health. The severity and duration of an air pollution episode depend on the pollutant, emissions intensity and meteorological conditions. Therefore, it is important to understand the mechanisms leading to these air pollution episodes.

Temperature inversions are one of the most crucial atmospheric conditions directly linked with stagnation episodes, favouring low horizontal and vertical dispersion of atmospheric pollutants. The combination of a thermal inversion and a high pressure system in addition to the increase in anthropogenic emissions lead to an increase in the aerosol and gaseous pollutants concentrations near the ground, and therefore to an increase in coagulation and condensation rates which results in large change in the aerosol size distribution (Wehner et al., 2002; Jacobson and Seinfeld, 2004; Janhäll et al., 2006). The strength and persistence of inversions and the characteristics of the atmospheric circulation during these conditions are affected by different factors like geographic location, regional and local topography and features of the urban area. Severe pollution conditions are also observed during stagnant anticyclonic conditions, which cause low wind-speeds and favour pollutant accumulation in the lower atmospheric layers (Lyamani et al., 2006a). Climate projections suggest that the frequency, intensity and duration of stagnation events (low wind speed and thermal inversion) are expected to increase in future, especially in Europe and North America (Forster et al., 2007). Under these extreme events the regional aerosol load and the concentrations of some gaseous pollutants can undergo pronounced increase, and thus lead to an increasing threat to human health.

This study focuses on the characterization of columnar and ground level aerosol properties during an extended stagnation event occurred in February 2011 at two urban sites, Granada and Málaga (South Spain). Additionally, the degree of compliance with the EU-legislated air quality standard for the different polluting agents measured at both sites is checked.

2. Experimental sites and instruments

Measurements used in this study were obtained during 1–20 February 2011 at two cities, Granada (37.16° N, 3.58° W, 680 m a.s.l.) and Málaga (36.72° N, 4.5° W, 40 m a.s.l.). Granada is a non-industrialized and medium sized city with 250,000 inhabitants. The city is located in a natural valley surrounded by mountains with elevations between 1000 and 3350 m a.s.l. Granada's climate is Mediterranean-continental with low temperatures in winter and high temperatures in summer. Major rainfall (361 mm yr^{-1}) occurs during winter and spring. Traffic (with a large proportion of diesel vehicles) is the most important source of anthropogenic pollutants in Granada (Lyamani et al., 2008, 2010). Domestic heating during winter (based on fuel oil combustion), is an additional pollutant source. The topography of Granada favours the development of thermal inversions in winter. Consequently, in combination with the emission of pollutants, this topography favours a significant accumulation of pollutants in the study area (Lyamani et al., 2008, 2010). Málaga is the major coastal city of the Andalusia region; it is located about 150 km Southeast of Granada. The population of the metropolitan area of Málaga is around 600,000 inhabitants. This city is located in the Mediterranean coast, bordered to the North by a high mountain range. The climate in Málaga is moderate, between temperate and warm and it has low rainfall (550 mm yr^{-1}). The local anthropogenic pollutant source is mainly traffic. Due to its location in the Mediterranean cost, one of the most important local meteorological systems affecting the air quality in Málaga area is the land-sea breeze (Millán et al., 1996).

Measurements of total columnar aerosol properties at day time were obtained using CIMEL CE-318 sun photometers at Málaga and Granada. Both instruments are part of the AERONET network (Holben et al., 1998; http://aeronet.gsfc.nasa.gov/). This instrument provides solar extinction measurements within the 340–1020 nm spectral range and sky radiance measurements at 440, 670, 870 and 1020 nm using the almucantar and principal plane configurations. The solar extinction measurements are used to compute the aerosol optical depth (AOD) at 340, 380, 440, 670, 870 and 1020 nm (Holben et al., 1998). The uncertainty in the retrieval of AOD under cloud free conditions is ±0.01 for wavelengths larger than 440 nm and ±0.02 for shorter wavelengths (Eck et al., 1999). The sky radiance measurements in conjunction with solar direct irradiance measurements at several wavelengths are used to retrieve aerosol microphysical properties like columnar aerosol size distribution, refractive index and single scattering albedo, $\omega_{0A}(\lambda)$, using the algorithm by Dubovik and King (2000) with improvements by Dubovik et al. (2006). In addition, the inversion code provides other parameters such as the volume concentration, modal radius and standard deviation for fine and coarse modes of the retrieved aerosol size distribution. For fine and coarse mode particles separation the inversion code finds the minimum within the size interval from 0.439 to 0.992 μm and uses this minimum as separation point between fine and coarse mode particles. The uncertainty of the AERONET inversion products is described by Dubovik et al. (2000). These authors showed that the uncertainty in the retrieval of $\omega_{0A}(\lambda)$ is ±0.03 for high aerosol load (AOD (440 nm) > 0.4) and solar zenith angle $> 50°$. For measurements with low aerosol load (AOD(440 nm) < 0.2), the retrieval accuracy of $\omega_{0A}(\lambda)$ drops down to 0.02–0.07 (Dubovik et al., 2000). For high aerosol load (AOD(440 nm) > 0.4) and solar zenith angle $> 50°$, errors are about 30%–50% for the imaginary part of the refractive index. Errors in aerosol size distribution retrievals dependent on particle size, aerosol type and actual values of the size distribution. For particles in the size range $0.1 < r < 7$ μm, retrieval errors are around 10–35%, while for sizes lower than 1 μm and higher than 7 μm retrieval errors rise up to 80–100%. In this work, the AERONET data of level 2 are used, unless otherwise indicated.

Columnar atmospheric aerosol properties during night time were obtained at Granada by a star photometer EXCALIBUR (Pérez-Ramírez et al., 2008). This instrument provides star extinction measurements at 380, 436, 500, 670, 880 and 1020 nm, which were used to compute the AOD at each wavelength using the methodology described by Pérez-Ramírez et al. (2011). Calibration of the instrument was performed twice a year in Calar Alto Astronomical Centre (37.2° N, 2.5° W, 2168 m a.s.l.) following Pérez-Ramírez et al. (2011). The spectral star photometer AOD was screened for clouds with the methodology developed by Pérez-Ramírez et al. (2012). The estimated uncertainty in the star photometer AOD is 0.02 for $\lambda < 800$ nm and 0.01 for $\lambda > 800$ nm (Pérez-Ramírez et al., 2011).

Moreover, the scattering coefficient (σ_{sp}) was measured with an integrating nephelometer (model 3563, TSI) at three wavelengths 450, 550 and 700 nm. Calibration of the nephelometer was carried out three-four times a year using CO_2 as high span gas and filtered air as low span gas. The last calibration before February 2011 was done on November 2010. Calibrations constants changed less than 2% between consecutive calibrations with negligible influence on the results. The averaging time was set to 5 min and the zero signal was measured hourly. The scattering data were corrected for truncation errors according to Anderson and Ogren (1998). Particle size distribution and concentration measurements were conducted by an Aerodynamic Particle Sizer (APS-3321, TSI). This instrument is an optical particle counter that measure particle diameter and aerosol concentration, in real time, in 52 nominal size bins in the 0.50–20 μm diameter range. Air sampling for all the optical instruments was obtained from the top of a stainless steel tube, 20-cm diameter and 5 m length located at about 15 m above the ground (Lyamani et al., 2008, 2010). Measurements were performed with no aerosol size cut-off and no heating was applied to the sampled air.

It is well known that the scattering by aerosol particles strongly depends on the relative humidity (RH) showing minimum variation for RH $<$ 50% and a sharp increase for RH $>$ 80% (Anderson and Ogren, 1998; Xu et al., 2002). From 1 to 13 February 2011, the relative humidity inside the nephelometer chamber was below 45% while after this period ranged from 30 to 60% with 95% of RH data below 50%. Thus, the scattering coefficient results presented here, especially those obtained from 1 to 13 February, can be considered not influenced by RH. On other hand, the APS does not provide RH measurements of the sampled air. However, as the temperature of the air sampled by the APS was higher than the sampled by the nephelometer, the RH inside the APS was below 60%. Thus, the APS results presented here can be also considered independent of RH.

Information about the duration and strength of temperature inversion episodes near the surface was obtained from the analysis of the vertical temperature profiles measured by a ground-based multi-frequency passive microwave radiometer (HATPRO, Radiometer Physics GmbH). In addition, troposphere ozone, O_3, carbon monoxide, CO, sulphur dioxide, SO_2, nitrogen oxides (NO, NO_2 and NO_x) and PM_{10} (particles with aerodynamic diameter below 10 μm) mass concentration data were used. These data were collected by the Andalusian air quality monitoring network at a suburban traffic influenced air quality station in Granada (37.19° N, 3.61° W) and at an urban traffic influenced air quality station in Málaga (Carranque; 36.72° N, 4.45° W) were also used.

3. Analysis and interpretation of results

3.1. Synoptic situation and atmospheric temperature profiles

The meteorological analysis of the studied period shows a synoptic situation mainly governed by high-pressure systems moving from the Atlantic to the Iberian Peninsula and the Mediterranean during the first two weeks of February 2011. From 14 to 18 February the Peninsula is slightly influenced by a low pressure system from the Northeast Atlantic, which declined its influence on 19 and 20 February. Fig. 1 shows the surface pressure at mean sea level for 9 and 14 February 2011 generated by NOAA Air Resources Laboratory (http://ready.arl.noaa.gov/). Fig. 1a is representative of the conditions prevailing from 5 to 13 February. Small pressure gradients took place over the Peninsula during these days coinciding with the period when the high-pressure system was located over Spain. This situation blocks the entry of air masses from the Atlantic and promotes stagnation conditions, reducing the ventilation of the atmosphere. The pressure gradient at the surface over the Iberian Peninsula was very low and consequently there was an absence of wind with cloudless and dry conditions. On 14 February the synoptic situation changed drastically with a low-pressure system centred over the North Atlantic, allowing the entry of clean Atlantic air masses in the Peninsula and leading to the end of the stagnation period (Fig. 1b). This synoptic situation was also associated with 35 mm accumulated rainfall from 14 to 17 February.

Fig. 2 shows a contour plot representing the atmospheric temperature profiles measured by the passive microwave radiometer from 7 to 13 February at Granada. Although temperature profiles at 15 min time-resolution are available up to 10,000 m a.g.l., only data for the first 1100 m a.g.l. are presented to highlight the characteristics of the lower atmosphere. During this period, atmospheric thermal inversions normally occurred from midnight until the first half of each day. The duration, height and severity of these thermal inversions varied widely among these days. Thermal inversion on 9 February was particularly long lasting (from 03:00 to

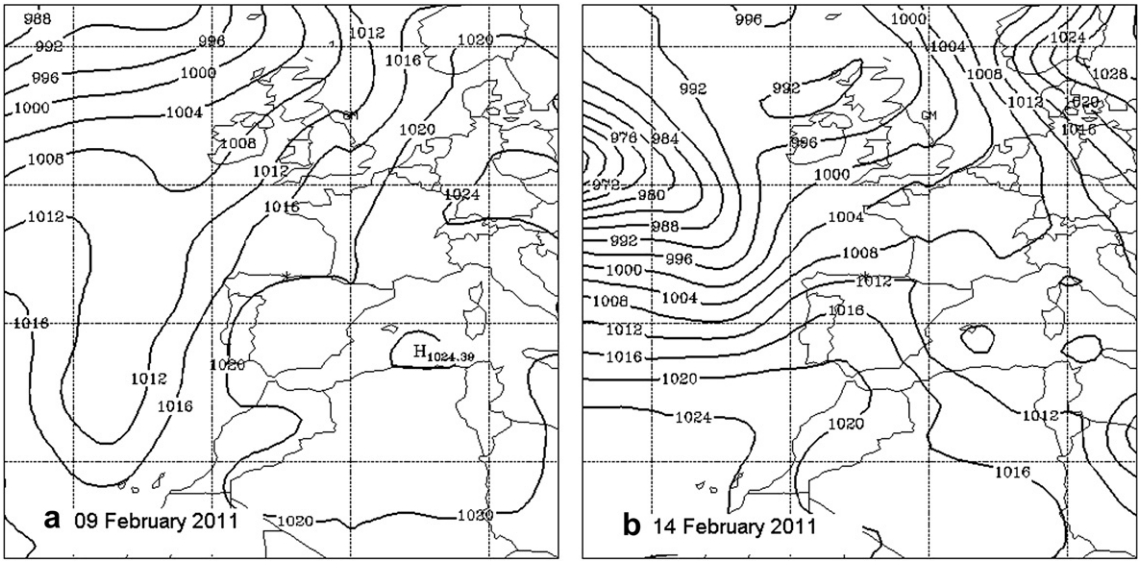

Fig. 1. Synoptic chart of surface pressure at mean sea level for 9 (a) and (b) 14 February 2011.

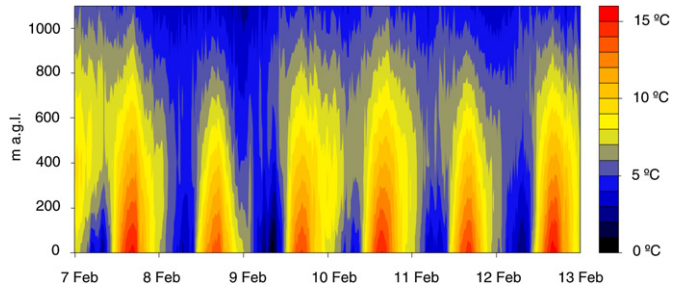

Fig. 2. Contour plot of the atmospheric temperature profiles up to 1100 m a.g.l. at Granada from 7 to 13 February 2011.

12:00 UTC) and severe (temperature at 740 m a.g.l. was nearly 5 K warmer than at surface level); extending until midday and with larger intensity at around peak morning traffic (8:15 UTC). Conversely, there were no thermal inversions in the first 3 days of February and from 4 to 6 there were less intense inversions (temperature at 700 m a.g.l. was 4 K warmer than at surface level, figure not shown) in the early morning compared to the ones observed from 7 to 13 February. On the other hand, the lower pressures affecting the Peninsula since 14 February promotes ventilation of the atmosphere, avoiding thermal inversion development during these days.

3.2. Atmospheric aerosol columnar characteristics

The AOD (440 nm) measured at Granada (day and night time) and at Málaga (day time) during 1–20 February 2011 have a similar temporal evolution as shown in Fig. 3. It can be noticed that there is a significant day-to-day variability in AOD (440 nm) at both sites: values registered in Málaga ranged from 0.05 to 0.50 and those from Granada varied from 0.05 to 0.60 at day time and 0.06 to 0.50 at night time. High values of AOD were observed during the long lasting event from 7 to 13 February at both sites with peak values between days 8 and 10. Moreover, it is important to note the increase in the minimum aerosol load from 7 to 13 February as compared with previous and following days. In fact, there is a fivefold increase in the minimum AOD, from approximately 0.05–0.25 on 6 and 9 February respectively. This large increase in AOD was associated to stagnation of air masses which favoured the accumulation of particles in the atmosphere and consequently produced an increase in AOD; particularly from 8 to 10 February. At the end of this episode the arrival of clean air masses from the Atlantic (Fig. 1b) produced a sharp decrease in AOD, reaching values close to those before the episode (<0.20).

Additional information on aerosol properties over the studied areas can be obtained from the analyses of the Angström exponent, α (Angström, 1929). This parameter is a basic measure of the aerosol size distribution; large values (around 2) indicate the prevalence of fine particles from urban-industrial and biomass burning sources, while low values of α (around 0) are related to coarse particles such as desert dust and marine aerosols (Dubovik et al., 2002). The Angström exponent α (440–870 nm) computed using AOD in the range 440–870 nm was used in this study. As in the case of AOD, α (440–870 nm) showed a similar pattern at both sites (Fig. 4). During the 7–13 February intense stagnation episode, α (440–870 nm) varied between 1.1 and 1.9 with a mean value of 1.6 ± 0.1 at Málaga during day time, while night time values (day time values) at Granada ranged from 1.1 to 2.0 (1–2) with a mean value of 1.8 ± 0.3 (1.7 ± 0.2). The large AOD in combination with the high α (440–870 nm) values are a clear indication of a large contribution of fine particles to the columnar atmospheric aerosol

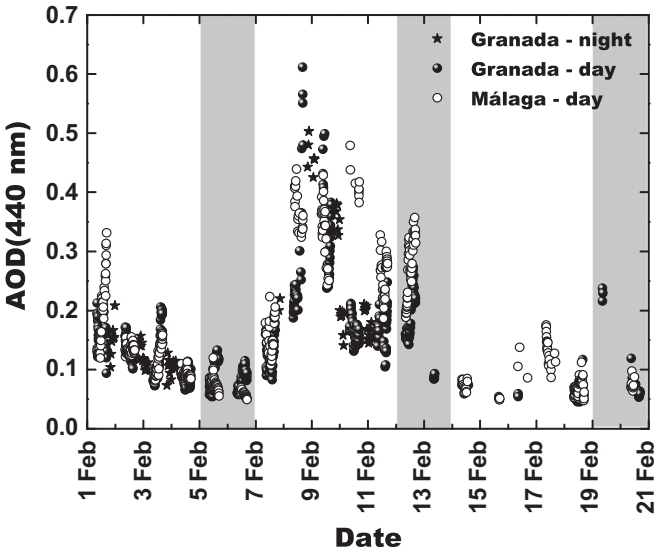

Fig. 3. Aerosol optical depth at 440 nm measured at Granada (during night and day time) and at Málaga (day time) from 1 to 20 February 2011. Shaded areas mark weekend days.

load during this episode. Similarly, high α (440–870 nm) values were observed at both sites before this intense event (from 1 to 6 February), also indicating the predominance of fine particles on these days; nevertheless the aerosol load was much lower than throughout the intense stagnation period. Since 14 February, there is a drastic change with a significant decrease in α (440–870 nm) down to values lower than 1, indicating a decrease in the contribution of aerosol fine particles to the aerosol load during this period.

The columnar aerosol volume size distributions obtained at Granada and Málaga from 1 to 13 February were bimodal with prevalence of fine mode particles, especially during the stagnation period. After 13 February, the retrieved aerosol size distributions at both sites were also bimodal but with predominance of coarse mode particles, in agreement with α (440–870 nm) values.

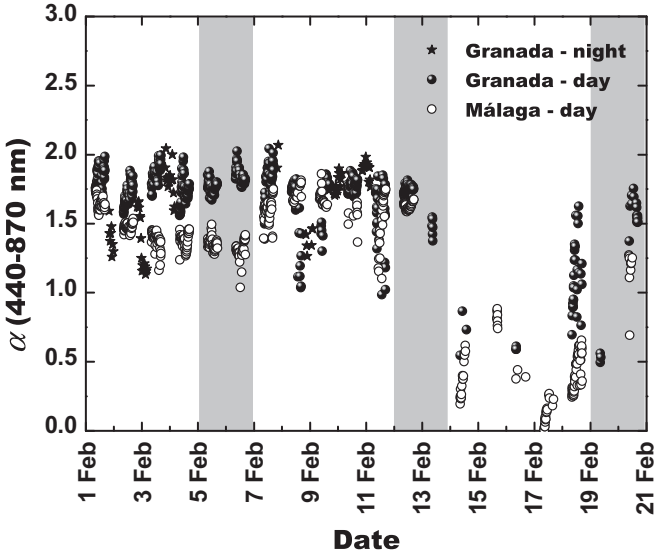

Fig. 4. Angström exponent, α (440–870 nm) measured at Granada (night and day time) and Málaga (day time) from 1 to 20 February 2011. Shaded areas mark weekend days.

Nevertheless, differences in the main features of aerosol size distributions (concentration, radius mode and the width of the fine and coarse modes) between the two cities, primarily due to the differences in aerosol source strength, were also observed. Other factor contributing to these differences are topography, wind speed, wind direction, relative humidity and temperature. Fig. 5 shows representative columnar aerosol volume size distributions for selected days before, during and after the intense stagnation episode at Málaga and Granada. Columnar volume size distributions show interesting features, evidencing the clear dominance and the large increase in the fine mode concentration at both sites during the intense stagnation episode. In fact, there was a significant increase in the fine mode concentration at both sites from values lower than 0.02 $\mu m^3\ \mu m^{-2}$ before 7 February to values up to 0.08 $\mu m^3\ \mu m^{-2}$ on days 8–10, and decreasing to previous values after 13 February. Its worth noting that the fine mode concentration values obtained at both sites during the intense stagnation episode are similar to those obtained by Lyamani et al. (2006b) at Granada during the severe heat wave that affected Western Europe during August 2003 (0.02–0.09 $\mu m^3\ \mu m^{-2}$). The shape of the size distributions, the location of the fine mode radius (0.17–0.20 μm) and the geometric standard deviation of the fine mode (~0.50) did not experience significant changes during the studied period at Málaga (Fig. 5a). Moreover, there was a good agreement with the climatology values of fine mode radius (0.12–0.21 μm) and the geometric standard deviation of the fine mode (0.38–0.46 μm) reported for urban industrial aerosol by Dubovik et al. (2002).

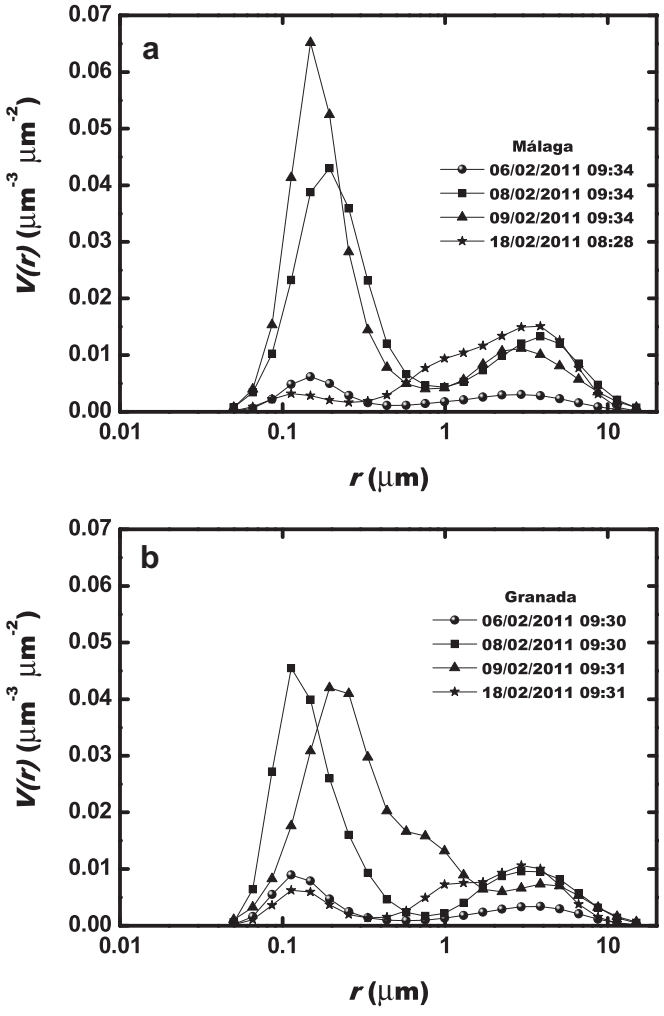

Fig. 5. Columnar aerosol volume size distribution obtained for selected days before, during and after the stagnation episode at Málaga (a) and Granada (b).

The most interesting result arising from the comparison of the fine mode size distributions obtained at Granada is the shift towards larger size particles in the morning hours on 9 February (Fig. 5b). There was a displacement of the fine mode radius from 0.15 μm before 9 February to 0.26 μm at 9:30 UTC on 9 February; at 13:30 UTC the fine mode radius goes back to the initial values as the previous days (figure not shown). In addition, the geometric standard deviation of the fine mode observed at Granada at 9:30 UTC on 9 February (0.63) was higher as compared to the rest of the days (0.45–0.50 μm). The fine mode radius obtained in the morning hours on 9 February at Granada (0.26 μm) is larger than the maximum value of 0.21 μm reported for urban-industrial aerosol (for AOD (440 nm) > 1) by Dubovik et al. (2002). This fine mode radius was similar to the one reported for high pollution episodes (with AOD (440 nm) > 1) at Anmyon Island in South Korea (Eck et al., 2005). Nevertheless, for AOD (440 nm) around 0.5, similar to the ones obtained at Granada during the morning hours on 9 February, the fine mode radius measured at Granada is much larger than the reported values by Dubovik et al. (2002) and Eck et al. (2005) for anthropogenic aerosol (0.17 μm). The geometric standard deviation of the fine mode size distribution in the morning hours on 9 February at Granada (0.63 μm) is also larger than reported values (0.38–0.46 μm) for urban-industrial aerosol (Dubovik et al., 2002). The combination of a high pressure system and a thermal inversion favouring low vertical and horizontal pollutants dispersion in addition to the increase in anthropogenic emissions (mostly from traffic) lead to an increase in the aerosol and gaseous pollutants concentrations near the ground, and therefore to an increase in coagulation and condensation rates which may explain the increase in radius and width of the fine mode size distributions at Granada in the morning hours on 9 February. The shift in the fine mode particle size to larger sizes observed in Granada on that day is not evidenced in Málaga (Fig. 5a), may be because the intensity of the thermal inversion at the Málaga coastal site was lower than at Granada.

The single scattering albedo, $\omega_{0A}(\lambda)$, is a key parameter for the estimation of the direct radiative impact of aerosols. This parameter is defined as the ratio of the scattering and the extinction coefficients. It depends on the relative source strengths of the various aerosol substances; purely scattering particles (e.g. sulphates) exhibit values of 1, while very strong absorbers (e.g. black carbon) can have values of 0.2 (Schnaiter et al., 2003). Due to the strong limitations imposed by the AERONET inversion algorithm (AOD (440 nm) > 0.4 and solar zenith angle > 50°) and the reduced sampling of sky radiances (almucantar sky radiance measurements at 1 h interval) as well as the presence of clouds during measurements, there was only one $\omega_{0A}(\lambda)$ level 2 retrieval at Granada, corresponding to the size distribution on 9 February shown in Fig. 5b. For the same reasons, there were no $\omega_{0A}(\lambda)$ retrievals in the level 2 category at Málaga. Thus, for comparing $\omega_{0A}(\lambda)$ values at both sites, the AERONET level 1.5 cloud screened $\omega_{0A}(\lambda)$ retrieved for Málaga at 9:34 UTC on 8 February, corresponding to size distribution shown in Fig. 5a, was used. The inversion retrieval in this case did not passed the AERONET level 2 threshold for aerosol load (AOD (440 nm) > 0.4) but it was just slightly lower (AOD (440 nm) = 0.39), while the solar zenith angle (66°) was above the AERONET threshold.

Fig. 6 shows the retrieved $\omega_{0A}(\lambda)$ values for Málaga and Granada on 8 and 9 February respectively. The spectral dependence of $\omega_{0A}(\lambda)$ obtained at Granada and Málaga were significantly different. The $\omega_{0A}(\lambda)$ values (at all wavelengths) in Málaga were lower than in Granada, indicative of a higher contribution of absorbing aerosol

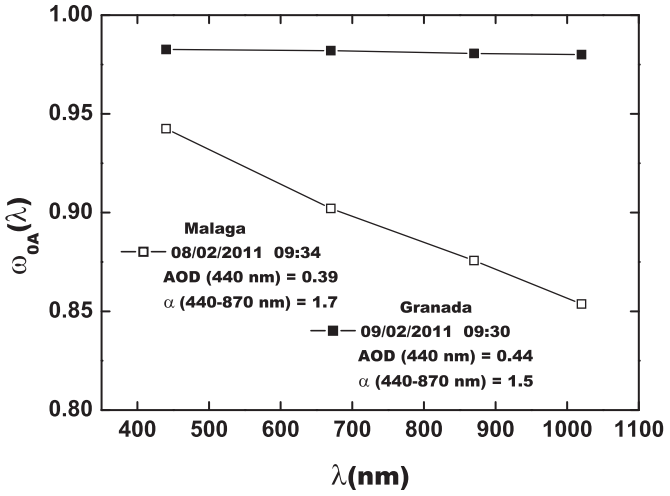

Fig. 6. Single scattering albedo retrieved for Granada and Málaga on 9 and 8 February respectively.

(especially black carbon) to the aerosol load in Málaga. As can be observed in Fig. 6, $\omega_{0A}(\lambda)$ for Málaga sharply decreased with wavelength from 0.94 at 440 nm to 0.85 at 1020 nm, according to the spectral variation characteristic of urban-industrial aerosols (Dubovik et al., 2002; Lyamani et al., 2006b). The retrieved $\omega_{0A}(\lambda)$ for Málaga are close to the reported values for urban-industrial aerosols by Dubovik et al. (2002) for Paris, France (0.94 at 440 nm and 0.91 at 1020 nm), Mexico City (0.90 at 440 nm and 0.83 at 1020 nm) and Maldives (0.91 at 440 nm and 0.84 at 1020 nm). These values are also in agreement with those obtained in Granada (0.91 at 440 nm and 0.83 at 1020 nm) under anthropogenic pollution conditions during the severe 2003 summer heat wave (Lyamani et al., 2006b). Conversely, $\omega_{0A}(\lambda)$ at Granada did not show the spectral variation (decrease with wavelength) characteristic of urban-industrial aerosols (Dubovik et al., 2002; Eck et al., 2005; Lyamani et al., 2006b). In fact, $\omega_{0A}(\lambda)$ for Granada shows neutral spectral dependence, which is the typical characteristic of desert dust (Dubovik et al., 2002). The imaginary refractive index in this case was low (0.002) with neutral spectral dependence. The $\omega_{0A}(\lambda)$ increasing with wavelength or with neutral spectral dependence are usually retrieved under dusty conditions at Granada (Lyamani et al., 2006b; Mladenov et al., 2011; Valenzuela et al., 2012a,b). In absence of desert dust or in situations dominated by anthropogenic or biomass burning particles, $\omega_{0A}(\lambda)$ usually shows a sharp decrease with wavelength at Granada (Lyamani et al., 2006b; Mladenov et al., 2011). Thus, the $\omega_{0A}(\lambda)$ neutral spectral behaviour observed at Granada may be due to the presence of desert dust over the study area. However, air-mass backward-trajectories from the HYSPLIT model (http://ready.arl.noaa.gov/HYSPLIT.php) show that at the time of the $\omega_{0A}(\lambda)$ retrieval on 9 February Granada was affected by European-Mediterranean air masses (source of anthropogenic aerosol) and that these air masses have not passed over North Africa (source of desert dust), indicating that the site was not influenced by the advection of desert dust from North Africa. This was also confirmed by TOMS and MODIS satellite images not showing desert dust over the area on 9 February. In addition, the columnar aerosol size distribution at the time of the $\omega_{0A}(\lambda)$ retrieval reveals the predominance of the fine mode (Fig. 5b) and no significant presence of desert dust (dominated by particles in the coarse mode) over Granada. The high $\omega_{0A}(\lambda)$ value (0.98) along with the flat spectral dependence at Granada result from the combination of nearly constant and low imaginary refractive index and the very large size and broad distribution of particles in the fine mode, which results in higher scattering efficiency in the 440–1020 nm range. Similar spectral $\omega_{0A}(\lambda)$ behaviour was observed by Eck et al. (2009) for biomass burning aerosols (dominated by fine particles) in Alaska and Bonanza (Greek) and was also attributed to large particle sizes in the fine mode.

3.3. Aerosol optical and physical properties at ground level

Aerosol optical and physical properties at ground level were only available at Granada. The particle number concentrations have been integrated from the number size distributions measured by the APS for two different intervals: the fine mode (aerodynamic diameter between 0.5 and 1.0 μm) and the coarse mode (aerodynamic diameter >1.0 μm). Fig. 7 shows hourly average values of the fine mode concentration (N_F) measured at surface level and the temperature gradient ($\Delta T/\Delta Z$) in the first 100 m a.g.l. during 1–20 February 2011. Positive and negative values of $\Delta T/\Delta Z$ correspond to thermal inversion and non inversion conditions respectively. As can be observed in Fig. 7, there were temperature inversions during the night and early morning from 1 to 13 February, with longer duration corresponding to days between 7 and 13 February. It is important to note that thermal inversions were more severe (higher $\Delta T/\Delta Z$) during weekends (Sunday 6 and 13 February). From 14 February there was a drastic change in the atmospheric conditions preventing the formation of thermal inversions within the following week.

Consequently, from 7 to 13 February the fine mode concentration at the surface showed a large increase in agreement with results from the entire atmospheric column. Moreover, there is a sharp enhance in N_F during days 8–10 as a result of the combination of severe thermal inversion in coincidence with peak traffic emission on these work days, particularly on 9 February when thermal inversion extended until 12:00 UTC. Before the stagnation episode, N_F had a mean value around 10 cm^{-3}, raising up to 85 cm^{-3} on 9 February and decreasing below 5 cm^{-3} after 13 February due to the entry of clean air masses from the Atlantic. Although there is a small increase in the coarse mode concentration (aerodynamic diameter >1.0 μm) at the surface around 9 February with a peak value on that day, the concentration for this mode does not show significant changes throughout the period (figure not shown). Before 13 February there was a predominance of fine particles and thereafter the contribution of coarse particles to aerosol load

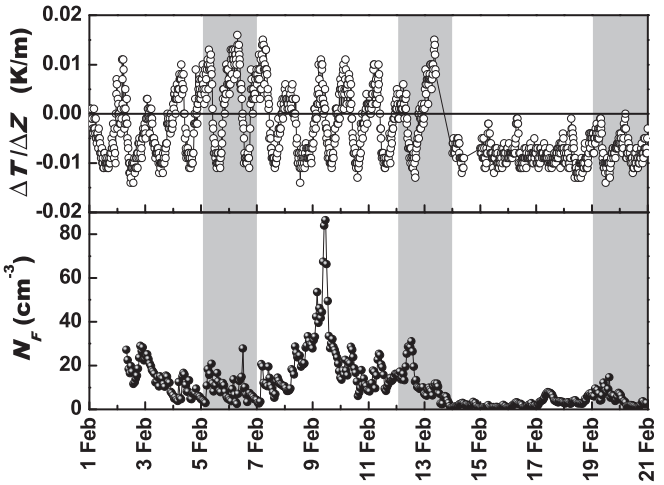

Fig. 7. Aerosol fine mode concentration (bottom) and atmospheric temperature gradient ($\Delta T/\Delta Z$) in the first 100 m a.g.l. (top) measured at Granada from 1 to 20 February 2011. Shaded areas mark weekend days.

increases at the surface due to a decrease in the fine particle concentration. Although thermal inversions were more severe on 6 and 13 February (weekend days), N_F was much lower than on 9 February. This is explained by the decrease in anthropogenic emissions to the atmosphere on weekend days (i.e. traffic emissions). In fact, Lyamani et al. (2010) already found a significant decrease in N_F during weekends compared to work days using 2-year data from Granada.

The drastic changes in the modal radius and concentration of the columnar fine mode particles observed in the morning hours on 9 February (Fig. 5b) were also evidenced by the analysis of the aerosol size distributions obtained in Granada at ground level by the APS. It is worth noting that the comparison of volume aerosol size distributions measured by the sun photometer and the APS may not be suitable due to instrumental, methodological and sampled air differences. Fig. 8 shows representative volume size distributions for 8 and 9 February 2011 derived from the number size distributions measured with the APS. Volume size distributions for the rest of the days showed similar shape (width and modal radius) to the one obtained on 8 February and therefore are not added to Fig. 8. Comparison of the fine mode size distributions on these dates revealed a significant shift towards larger size particles and an increase in the width of the fine mode distributions on 9 February. In fact, the fine modal radius for these cases shifted from 0.30 to 0.35 μm on 8 February to 0.64 μm on 9 February. As previously indicated, changes in the fine mode characteristics (magnitude, width and modal radius) on 9 February are attributed to growth mechanisms such as coagulation and condensation.

In relation to the aerosol scattering coefficient, σ_{sp} (550 nm), and scattering Angström parameter, α_s (450–700 nm), computed using σ_{sp} in the 450–700 nm range; Fig. 9 shows values corresponding to the monitoring period. Aerosol scattering coefficients at 450 and 700 nm showed similar temporal evolutions as σ_{sp} (550 nm). It can be observed that σ_{sp} (550 nm) follows a similar pattern as the fine mode concentration with high values during the intense stagnation period (7–13 February) and low values thereafter. The highest σ_{sp} (550 nm) values (maximum 460 Mm^{-1}) were reached as in the case of N_F on 9 February, when the long lasting thermal inversion occurred. Conversely, the lower σ_{sp} (550 nm) values were measured after 13 February (mainly below 20 Mm^{-1}), when the Atlantic air mass advections in association with rain produced a high decrease in particle load and therefore a significant decrease in σ_{sp} (550 nm). From 1 to 13 February, the α_s (450–700 nm) values were rather high with values above 1.5, indicating the predominance of fine particles during the episode, also in agreement with the surface size distribution results. After 13 February, α_s (450–700 nm) showed a significant decrease indicating a decrease in the contribution of aerosol fine particles during this period. It is interesting to note that α_s (450–700 nm) and α (440–870 nm) showed similar temporal evolution during the entire period, indicative of the strong contribution of aerosol at ground level to the entire atmospheric column.

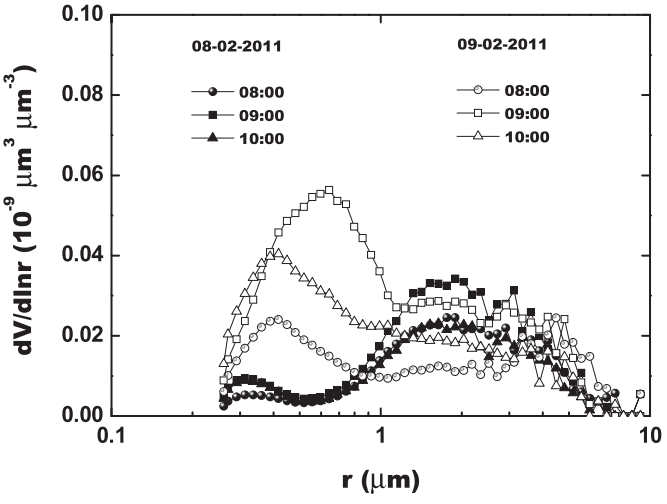

Fig. 8. Aerosol volume size distributions at ground level measured by the Aerosol Particle Sizer in Granada on 8 and 9 February 2011.

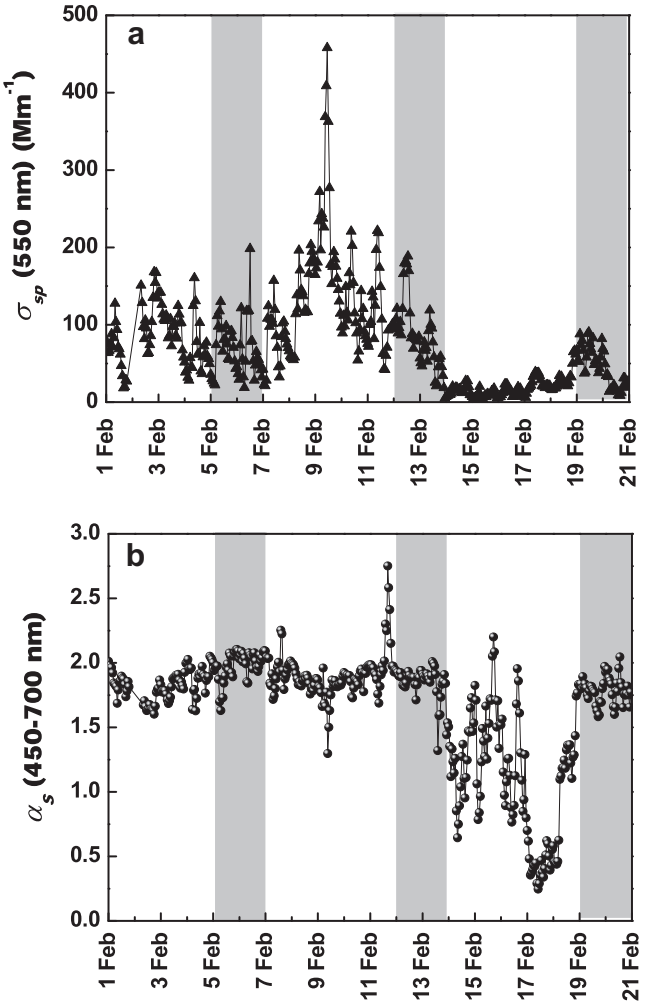

Fig. 9. Aerosol scattering coefficient at 550 nm (a) and scattering Angström parameter (b) measured at Granada from 1 to 20 February 2011. Shaded areas mark weekend days.

3.4. Air quality

Fig. 10 shows the temporal evolution of daily PM_{10} mass concentration values at Granada and Málaga from 1 to 20 February 2011 where the horizontal line indicates the PM_{10} mass concentration European daily limit. PM_{10} mass concentration ranged from 8 to 63 and 10–95 μg m^{-3} at Málaga and Granada respectively; these values are in the range of values obtained in other Spanish urban areas (Querol et al., 2008), but slightly higher if compared to other European cities (Putaud et al., 2010). During the stagnation period, PM_{10} mass concentration at Granada and Málaga were relatively high as compared to non-stagnation days. In fact, the daily limit value of 50 μg m^{-3} fixed by the European directive

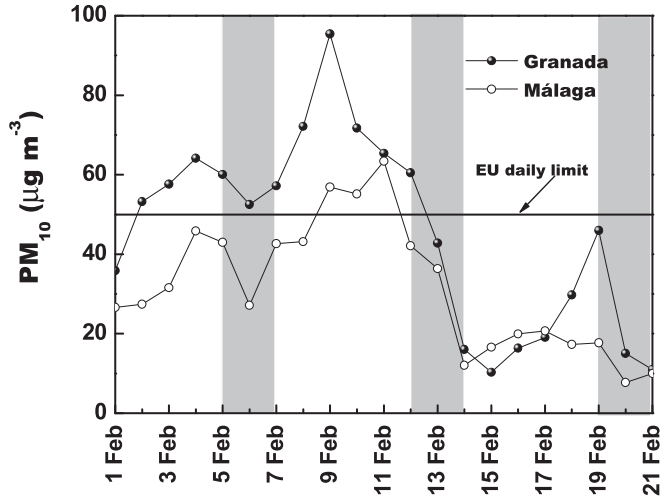

Fig. 10. Daily PM_{10} mass concentration values at Granada and Málaga from 1 to 20 February 2011. Dashed area marks weekend days and the horizontal line shows the PM_{10} mass concentration European daily limit.

(2008/50/CE) was exceeded in Granada from 2 to 12 February and in Málaga from 9 to 11 February.

Moreover, during the stagnation period, the concentrations of SO_2, NO_2 and CO were relatively high at Granada and Málaga as compared to non-stagnation days. On the contrary, O_3 concentration showed a drastic decrease during 1–13 February at both sites. This decrease was directly related to the increase in the destruction rate of O_3 due to presence of high concentration of NO_x and aerosol particles next to the surface favoured by high pressure systems and thermal inversions (below 700 m a.g.l.) during these days. The O_3 maximum hourly concentration was 95 and 102 μg m^{-3} at Granada and Málaga respectively, always below the threshold value set by the EU directive (180 μg m^{-3}). The increasing pattern for gaseous pollutants has been previously observed at other sites in association with both the traffic emission pattern and the stabilization and height of the boundary layer (Charron and Harrison, 2003; Janhäll et al., 2004). Nevertheless, although there was an increase in the concentration of SO_2, NO_2 and CO during the stagnation episode, maximum-hourly average concentrations for these gaseous pollutants were 47, 179 and 1911 μg m^{-3} at Granada, and 14, 160 and 1327 μg m^{-3} at Málaga respectively; always below the threshold values set by the EU directive 2008/50/EC (350, 200 and 10,000 μg m^{-3} respectively).

4. Conclusions

Continuously tropospheric temperature profiles monitored at Granada by means of a ground-based multiple-channel microwave radiometer from 1 to 20 February 2011 revealed the presence of morning temperature inversions from 4 to 13 February with larger duration and intensity during 7–13 February. This long lasting event was associated with a very strong and persistent blocking high-pressure system over the Iberian Peninsula. Columnar and in situ aerosol optical and physical properties measured at two urban sites with varying emission characteristics and atmospheric conditions, Granada and Málaga (South Spain, AERONET sites), were analysed to characterize aerosol properties before, during and after this extended stagnation episode. Pronounced enhancement in columnar aerosol optical depth was observed at both sites throughout this event, indicating its large spatial extension and strong impact on the regional aerosol properties. Moreover, a significant increase in the aerosol scattering coefficients and aerosol fine number concentrations at ground level were observed at Granada during this stagnation episode. Furthermore, columnar aerosol volume size distributions obtained at Granada and Málaga during 1–13 February were bimodal with prevalence of fine mode particles, especially during the stagnation period. After 13 February, the retrieved aerosol size distributions at both sites were also bimodal but with predominance of coarse mode particles, in agreement with Angström exponent values. Nevertheless, differences in the main features of aerosol size distributions between the two cities, due to the differences in aerosol source strength as well as local atmospheric conditions, were also observed. The fine mode size distributions at Granada showed a displacement towards larger size particles together with an increase in the geometric standard deviation of the fine mode in the morning hours on 9 February due to coagulation and condensation processes. Single scattering albedo in this case was higher and showed a neutral spectral dependence, in contrast to the usual spectral dependence reported for anthropogenic pollution particles at this site. During the stagnation period, the SO_2, CO, NO_2 and PM_{10} mass concentrations measured at both sites were relatively high as compared to non-stagnation days, with a decrease in O_3 mass concentrations at both sites. Only the European PM_{10} mass concentration limit (50 μg m^{-3}) was exceeded in Granada for most days and in Málaga for three consecutive days. The decrease in anthropogenic activities during weekend days (i.e. traffic emissions) decreases the impact of the severe thermal inversions on 6 and 13 February.

Acknowledgements

This work was supported by the Spanish Ministry of Science and Technology through projects CGL2010-18782 and CSD2007-00067; by the Andalusian Regional Government through projects P10-RNM-6299 and P08-RNM-3568; and by EU through ACTRIS project (EU INFRA-2010-1.1.16-262254). The authors would like to express their gratitude to the NOAA Air Resources Laboratory and Naval Research Laboratory for providing the meteorological maps. The authors would also like to thank the anonymous reviewers for their constructive comments that have helped to improve the manuscript.

References

Anderson, T.L., Ogren, J.A., 1998. Determining aerosol radiative properties using the TSI 3563 integrating nephelometer. Aerosol Science and Technology 29, 57–69.
Angström, A., 1929. On the atmospheric transmission of sun radiation and on dust in the air. Geografiska Annaler 11, 156–166.
Charron, A., Harrison, R.M., 2003. Primary particle formation from vehicle emissions during exhaust dilution in the roadside atmosphere. Atmospheric Environment 37, 4109–4119.
Choi, H., Zhang, Y.H., Kim, K.H., 2008. Sudden high concentration of TSP affected by atmospheric boundary layer in Seoul metropolitan area during dust storm period. Environment International 34, 635–647.
Dubovik, O., King, M.D., 2000. A flexible inversion algorithm for retrieval of aerosol optical properties from sun and sky radiance measurements. Journal of Geophysical Research 105, 20673–20696.
Dubovik, O., Smirnov, A., Holben, B.N., King, M.D., Kaufman, Y.J., Eck, T.F., Slutsker, I., 2000. Accuracy assessments of aerosol optical properties retrieved from AERONET sun and sky-radiance measurements. Journal of Geophysical Research 105, 9791–9806.
Dubovik, O., Holben, B., Eck, T.F., Smirnov, A., Kaufman, Y.J., King, M.D., Tanré, D., Slutsker, I., 2002. Variability of absorption and optical properties of key aerosol types observed in worldwide locations. Journal of the Atmospheric Sciences 59, 590–608.
Dubovik, O., Sinyuk, A., Lapyonok, T., Holben, B.N., Mishchenko, M., Yang, P., Eck, T.F., Volten, H., Munoz, O., Veihelmann, B., van der Zander, W.J., Leon, J.F., Sorokin, M., Slutsker, I., 2006. Application of spheroid models to account for aerosol particle nonsphericity in remote sensing of desert dust. Journal of Geophysical Research 111, D11208.
Eck, T.F., Holben, B.N., Reid, J.S., Dubovik, O., Smirnov, A., O'Neill, N.T., Slutsker, I., Kinne, S., 1999. Wavelength dependence of the optical depth of biomass burning, urban, and desert dust aerosol. Journal of Geophysical Research 104, 31333–31349.

Eck, T.F., Holben, B.N., Dubovik, O., Smirnov, A., Goloub, P., Chen, H.B., Chatenet, B., Gomes, L., Zhang, X.-Y., Tsay, S.-C., Ji, Q., Giles, D., Slutsker, I., 2005. Columnar aerosol optical properties at AERONET sites in central eastern Asia and aerosol transport to the tropical mid-Pacific. Journal of Geophysical Research 110, D06202.

Eck, T.F., Holben, B.N., Reid, J.S., Sinyuk, A., Hyer, E.J., O'Neill, N.T., Shaw, G.E., Van de Castle, J.R., Chapin, F.S., Dubovik, O., Smirnov, A., Vermote, E., Schafer, J.S., Giles, D., Slutsker, I., Sorokine, M., Newcomb, W.W., 2009. Optical properties of boreal region biomass burning aerosols in central Alaska and seasonal variation of aerosol optical depth at an Arctic coastal site. Journal of Geophysical Research 114, D11201.

Fisher, B.E.A., Kukkonen, J., Schatzmann, M., 2001. Meteorology applied to urban air pollution problems COST 715. International Journal of Environment and Pollution 16, 560–570.

Forster, P., Ramaswamy, V., Artaxo, P., Berntsen, T., Betts, R., Fahey, D.W., Haywood, J., Lean, J., Lowe, D.C., Myhre, G., Nganga, J., Prinn, R., Raga, G., Schulz, M., Dorland, R.V., 2007. Changes in atmospheric constituents and in radiative forcing. Climate change 2007: the physical science basis. In: Solomon, S., Qin, D., Manning, M., Chen, Z., Marquis, M., Averyt, K.B., Tignor, M., Miller, H.L. (Eds.), Contribution of Working Group I to the Fourth Assessment Report of the Intergovernmental Panel on Climate Change.

Holben, B.N., Eck, T.F., Slutsker, I., Tanré, D., Buis, J.P., Setzer, A., Vermote, E., Reagan, J.A., Kaufman, Y.J., Nakajima, T., Lavenu, F., Jankowiak, I., Smirnov, A., 1998. Aeronet- a federated instrument network and data archive for aerosol characterization. Remote Sensing of Environment 66, 1–16.

Jacobson, M.Z., Seinfeld, J.H., 2004. Evolution of nanoparticle size and mixing state near the point of emission. Atmospheric Environment 38, 1839–1850.

Janhäll, S., Jonsson, Å.M., Molnár, P., Svensson, E.A., Hallquist, M., 2004. Size resolved traffic emission factors of submicrometer particles. Atmospheric Environment 38, 4331–4340.

Janhäll, S., Olofson, K.F.G., Andersson, P.U., Pettersson, J.B.C., Hallquist, M., 2006. Evolution of the urban aerosol during winter temperature inversion episodes. Atmospheric Environment 40, 5355–5366.

Lyamani, H., Olmo, F.J., Alcantara, A., Alados-Arboledas, L., 2006a. Atmospheric aerosols during the 2003 heat wave in southeastern Spain I: spectral optical depth. Atmospheric Environment 40, 6453–6464.

Lyamani, H., Olmo, F.J., Alcántara, A., Alados-Arboledas, L., 2006b. Atmospheric aerosols during the 2003 heat wave in southeastern Spain II: microphysical columnar properties and radiative forcing. Atmospheric Environment 40, 6465–6476.

Lyamani, H., Olmo, F.J., Alados-Arboledas, L., 2008. Light scattering and absorption properties of aerosol particles in the urban environment of Granada, Spain. Atmospheric Environment 42, 2630–2642.

Lyamani, H., Olmo, F.J., Alados-Arboledas, L., 2010. Physical and optical properties of aerosols over an urban location in Spain: seasonal and diurnal variability. Atmospheric Chemistry and Physics 10, 239–254.

Millán, M., Salvador, R., Mantilla, E., Artnano, B., 1996. Meteorology and photochemical air pollution in Southern Europe: experimental results from EC research projects. Atmospheric Environment 30, 1909–1924.

Mladenov, N., Alados-Arboledas, L., Olmo, F.J., Lyamani, H., Delgado, A., Molina, A., Reche, I., 2011. Applications of optical spectroscopy and stable isotope analyses to organic aerosol source discrimination in an urban area. Atmospheric Environment 45, 1960–1969.

Pérez-Ramírez, D., Aceituno, J., Ruiz, B., Olmo, F.J., Alados-Arboledas, L., 2008. Development and calibration of star photometry to measure the aerosol optical depth: smoke observations at a high mountain site. Atmospheric Environment 42, 2733–2738.

Pérez-Ramírez, D., Lyamani, H., Olmo, F.J., Alados-Arboledas, L., 2011. Improvements in star photometry for aerosol characterizations. Journal of Aerosol Science 42, 737–745.

Pérez-Ramírez, D., Lyamani, H., Navas-Guzmán, F., Olmo, F.J., Alados-Arboledas, L., 2012. Cloud screening and quality control algorithm for star photometer data: assessment with lidar measurements and with all-sky-images. Atmospheric Measurement Techniques 5, 1585–1599.

Putaud, J.P., Van Dingenen, R., Alastuey, A., Bauer, H., Birmili, W., Cyrys, J., Flentje, H., Fuzzi, S., Gehrig, R., Hansson, H.C., Harrison, R.M., Herrmann, H., Hitzenberger, R., Hüglin, C., Jones, A.M., Molnar, A., Moreno, T., Pekkanen, J., Perrino, C., Pitz, M., Puxbaum, H., Querol, X., Rodriguez, S., Salma, I., Schwarz, J., Smolik, J., Schneider, J., Spindler, G., ten Brink, H., Tursic, J., Viana, M., Wiedensohler, A., Raes, F., 2010. A European aerosol phenomenology – 3: physical and chemical characteristics of particulate matter from 60 rural, urban, and kerbside sites across Europe. Atmospheric Environment 44, 1308–1320.

Querol, X., Alastuey, A., Moreno, T., Viana, M.M., Castillo, S., Pey, J., Rodríguez, S., Artiñano, B., Salvador, P., Sánchez, M., Garcia Dos Santos, S., Herce Garraleta, M.D., Fernandez-Patier, R., Moreno-Grau, S., Negral, L., Minguillón, M.C., Monfort, E., Sanz, M.J., Palomo-Marín, R., Pinilla-Gil, E., Cuevas, E., de la Rosa, J., Sánchez de la Campa, A., 2008. Spatial and temporal variations in airborne particulate matter (PM_{10} and $PM_{2.5}$) across Spain 1999–2005. Atmospheric Environment 42, 3964–3979.

Schnaiter, M., Horvath, H., Möhler, O., Naumann, K.H., Saathoff, H., Schöck, O.W., 2003. UV-VIS-NIR spectral optical properties of soot and soot-containing aerosols. Journal of Aerosol Science 34, 1421–1444.

Valenzuela, A., Olmo, F.J., Lyamani, H., Antón, M., Quirantes, A., Alados-Arboledas, L., 2012a. Analysis of the desert dust radiative properties over Granada (2005–2010) using principal plane sky radiances and spheroids retrieval procedure. Atmospheric Research 104–105, 292–301.

Valenzuela, A., Olmo, F.J., Lyamani, H., Antón, M., Quirantes, A., Alados-Arboledas, L., 2012b. Classification of aerosol radiative properties during African desert dust intrusions over southeastern Spain by sector origins and cluster analysis. Journal of Geophysical Research 117, D06214.

Wehner, B., Birmili, W., Gnauk, T., Wiedensohler, A., 2002. Particle number size distributions in a street canyon and their transformation into urban-air background: measurements and a simple model study. Atmospheric Environment 36, 2215–2223.

Xu, J., Bergin, M.H., Yu, X., Liu, G., Zhao, J., Carrico, C.M., Baumann, K., 2002. Measurement of aerosol chemical, physical and radiative properties in the Yangtze delta region of China. Atmospheric Environment 36, 161–173.